Medicinal Chemistry Research (2019) 28:1425–1440
https://doi.org/10.1007/s00044-019-02382-w

MEDICINAL CHEMISTRY RESEARCH

ORIGINAL RESEARCH

Cytotoxicity of multicellular cancer spheroids, antibacterial, and antifungal of selected sulfonamide derivatives coupled with a salicylamide and/or anisamide scaffold

Alaaeldin M. F. Galal[1] · Walid Fayad[2] · Walaa S. A. Mettwally[3] · Sanaa K. Gomaa[3] · Esam R. Ahmed[4] · Heba A. El-Refai[3] · Atef G. Hanna[1]

Received: 8 March 2019 / Accepted: 5 June 2019 / Published online: 14 June 2019

Abstract

In an attempt to overcome the drawbacks of the cancer monolayers model (2D), the 3-dimensional (3D) multicellular cancer spheroids (MCS) have been developed. Nine of most active sulfonamide derivatives coupled with a salicylamide scaffold were screened for cytotoxicity on two human cancer cell line spheroids (MCF7 and HCT116) in addition to one human normal cell line spheroid (RPE-1). 5-Chloro-*N*-[(*N*-4-chlorophenyl) 4-sulfamoylbenzyl] salicylamide (**9**) was found to be the most active compound among all tested compounds. It showed 70% inhibition on HCT116 spheroids, almost double the activity of cisplatin, and higher activity than cisplatin on MCF7 spheroids. Also, 5-chloro-*N*-[(*N*-benzyl) 4-sulfamoylbenzyl] salicylamide (**18**) and 5-chloro-*N*-[(*N*-2-phenylethyl) 4-sulfamoylbenzyl] salicylamide (**19**) showed cytotoxicity against HCT116 slightly lower than that of cisplatin (32% and 31%, respectively) but with much lower cytotoxicity against the normal cell (4% and 10% vs. 39%, respectively). Based on in silico virtual screening against DHPS enzyme, some sulfonamide derivatives coupled with a salicylamide and/or anisamide scaffold were tested in vitro against four bacterial and fungal pathogens. 5-Chloro-*N*-[(*N*-2-nitro-4-methylphenyl) 4-sulfamoylbenzyl] salicylamide (**17**) and 5-chloro-*N*-[(*N*-2-nitro-4-methylphenyl) 4-sulfamoylbenzyl] anisamide (**5**) showed strong antifungal activity on the tested organism, while the first one (**17**) have the strongest antibacterial activity against the G +ve and G −ve bacterium. In vitro, dihydropterate synthase (DHPS) enzyme assay showed that, compounds **5** and **17** effectively inhibit dihydropterate synthase (DHPS) enzyme by 93.78% and 95.15%, respectively, while miconazole inhibit the enzyme with only 87.50%. In addition, their effect upon amylase, lipase and protease enzymes was reported. The most active compounds **5**, **9**, **17–19** could be subjected to in vivo investigation as new drugs.

Supplementary information The online version of this article (https://doi.org/10.1007/s00044-019-02382-w) contains supplementary material, which is available to authorized users.

✉ Alaaeldin M. F. Galal
alaa17767@yahoo.com

[1] Chemistry of Natural Compounds Department, Pharmaceutical and Drug Industries Research Division, National Research Centre, 33 El Bohouth St. (former El Tahir St.)—Dokki, Giza P.O. 12622, Egypt

[2] Drug Bioassay-Cell Culture Laboratory, Pharmacognosy Department, National Research Centre, Dokki, Giza 12622, Egypt

[3] Chemistry of Natural and Microbial Products Department, Pharmaceutical and Drug Industries Research Division, National Research Centre, 33 El Bohouth St. (former El Tahir St.)—Dokki, Giza P.O. 12622, Egypt

[4] Confirmatory Diagnostic Unit, Vacsera, Giza, Egypt

Graphical Abstract

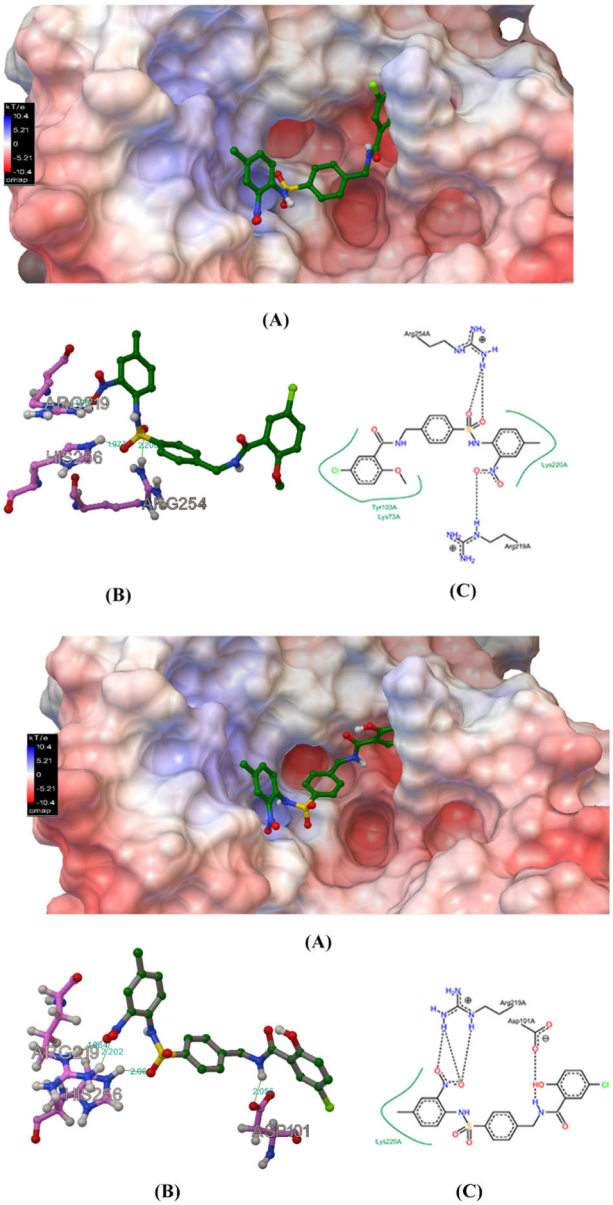

Keywords Cytotoxicity · Multicellular cancer spheroids · Sulfonamides · Antimicrobial · DHPS inhibitors.

Introduction

Multicellular cancer spheroids

The most prominent in vitro model for evaluating the anticancer activity of tested compounds is the cancer monolayers model (Zanoni et al. 2016). However, accumulated literatures reveal that active compounds on these monolayers most often show poor activity in cancer animal models or subsequent clinical trials (Hay et al. 2014). The failure of monolayers to accurately prediction, the in vivo activity can be attributed to the lack of complexity and different characteristics of in vivo solid tumor (Lee et al. 2007). In an attempt to overcome the drawbacks of the 2D model, the 3-dimensional (3D) multicellular cancer spheroids (MCS) have been developed (Sutherland et al. 1971). During the last decade, the interest in applying MCS in the evaluation of antitumor effect has been substantially increased (Galateanu et al. 2016).

The reason behind this is that the MCS mimic many aspects of the clinically diagnosed solid tumor. Main examples are 3D architecture (Lee et al. 2008), gene expression (Smith et al. 2012), growth kinetics (Wallace and Guo 2013), presence of hypoxic—known to be resistant—subpopulation (Wenzel et al. 2014), microenvironment (Baker and Chen 2012; Ekert et al. 2014) and extracellular matrix (Kimlin et al. 2013). In addition, MCS select for penetrating compounds into the tumor mass, which is an essential property for a clinically successful chemotherapeutic agent (Tunggal et al. 1999; Tannock et al. 2002).

Indeed, reports indicate the correlation between activity on MCS and in vivo models (Kobayashi et al. 1993; Kim et al. 2010). Thus, MCS model can more precisely predict the anticancer efficacy of the tested compounds compared to monolayers model.

Consequently, nine of the most active compounds, previously reported by us (Galal et al. 2018), were screened for cytotoxicity on two human cancer cell lines: MCF7, HCT116 (breast and colon carcinoma, respectively) and one normal human cell line: RPE-1 (retinal epithelial), all were grown as MCS. The RPE-1 was used to determine the safety of the tested compounds to normal cells, and thus, their selective cytotoxicity toward cancer cells.

Antibacterial and antifungal activities

Recently, antimicrobial drugs characterized with their selective toxicity. They kill or inhibit the growth of microbial targets selectively, while causing minimal or no harm to the host. Each class of antibacterial drugs has a unique mode of action such as cell wall biosynthesis inhibitors, protein synthesis inhibitors, membrane function inhibitors, nucleic acid synthesis inhibitors and metabolic pathway inhibitors (Supuran et al. 2002). The biosynthesis of folate derivatives is an attractive metabolic pathway for the development of new therapeutic compounds against infectious diseases caused by bacteria, fungi and some species of protozoa, as well as for some human diseases, including cancer and rheumatoid arthritis (McGuire 2003; Hawser et al. 2006; Gangjee et al. 2007).

A great difference between prokaryotes and eukaryotes are their mechanism for folate obtaining. Eukaryotes, essentially, require to uptake it from the media, while prokaryotes have de novo biosynthesis of folate in multistep mechanism (Hanson and Gregory 2011). The folate biosynthesis in microorganisms starts with the synthesis of the pterin ring, which is catalyzed by GTP cyclohydrolase I (GTPCHI). This enzyme is responsible for the hydrolysis of guanosine triphosphate (GTP) to form 7,8-dihydroneopterin triphosphate. The latter compound was catalyzed with two distinct enzymes to form hydroxymethyl-7,8-dihydropterin pyrophosphate (DHPPP) (Bertacine Dias et al. 2018). In this step, the attachment of *p*-amino benzoic acid (*p*ABA) to pterin moiety of DHPPP is catalyzed with dihydropteroate synthase enzyme (DHPS) to form 7,8-dihydropteroate. The addition of one or more glutamates moieties to 7,8-dihydropteroate was catalyzed with mono/dihydrofolate synthase and the bifunctional folylpoly-γ-glutamate synthase (DHFS/FPGS) enzymes to producing dihydrofolate and its derivatives. The reduction of latter compound to tetrahydrofolate was catalyzed with dihydrofolate reductase (DHFR) enzyme (Bertacine Dias et al. 2018). The last two steps of the pathway, which was catalyzed with DHPS and DHFR, have been used as antimicrobial or human disease targets (McGuire 2003; Hawser et al. 2006). Moreover, DHPS is one of the most studied enzymes of folate pathway since it is the target of sulfa drugs.

Sulfa drugs are very important class of antimicrobial drugs since it inhibit the growth of bacteria by competitively inhibiting the utilization of *p*ABA for the biosynthesis of folic acid. This class of compounds have extensive biological activities revolutionized the field of medical sciences (Ali et al. 2006). They were reported to be used as antitumor (Hanan et al. 2008; Chiarino et al. 1988; Owa et al. 1999; Owa et al. 2002; Mohan et al. 2006; Procopiou et al. 2013), antiallergic (Owa et al. 2002), antiparasitic (Lee et al. 2013), anti-inflammatory (Sulfasalazine) (Galiana-Roselló et al. 2013), antidiabetic (Tolbutamide) (Keche et al. 2012; Tang et al. 2013), neuroleptic (Thiothixene) (Höhn et al. 1973), diuretic (Furosemide), analgesic (Celecoxib), and antibacterial (Sulfanilamide derivatives) (Davie et al. 2013; Wilkinson et al. 2007; Weidel et al. 2013; Poręba et al. 2015).

In recent years, the increasing of resistance of some microbial strain to most of the antimicrobial drugs encouraged us to investigate the sulfonamide derivatives, previously synthesized by us (Galal et al. 2018), as new therapeutic agents against DHPS enzyme. At first, the sulfonamide derivatives coupled with a salicylamide and/or anisamide scaffold subjected to virtual screening against DHPS enzyme. Derivatives that docked into the pterin binding pocket and have acceptable binding affinity were re-synthesized and tested in vitro against some bacterial and fungal pathogens. Moreover, their effect upon amylase, lipase and protease enzymes was studied.

Results and discussion

Antitumor activity of the selected compounds

In the current study, MCS were used as the primary platform for evaluating the anticancer activity of the tested compounds. MCS represent an optimized cell based approach as they mimic the in vivo tumor environment

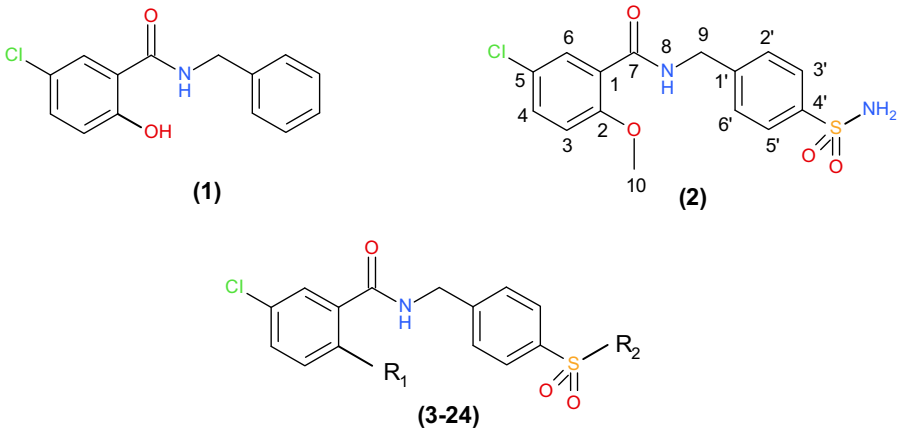

3: R_1=OCH_3, R_2=NH-(4-CH_3)Ph
4: R_1=OCH_3, R_2=NH-(4-OCH_3)Ph
5: R_1=OCH_3, R_2=NH-(2-NO_2-4-CH_3)Ph
6: R_1=OCH_3, R_2=NH-2-(1,3-thiazolyl)
7: R_1=OCH_3, R_2=piperazinyl
8: R_1=OH, R_2=NH-Ph
9: R_1=OH, R_2=NH-(4-Cl)Ph
10: R_1=OH, R_2=NH-(4-F)Ph
11: R_1=OH, R_2=NH-(4-CH_3)Ph
12: R_1=OH, R_2=NH-(4-OCH_3)Ph
13: R_1=OH, R_2=NH-(4-NH_2)Ph
14: R_1=OH, R_2=NH-(4-OH)Ph
15: R_1=OH, R_2=NH-(2-OH)Ph
16: R_1=OH, R_2=NH-(2-COOH)Ph
17: R_1=OH, R_2=NH-(2-NO_2-4-CH_3)Ph
18: R_1=OH, R_2=NH-CH_2-Ph
19: R_1=OH, R_2=NH-$(CH_2)_2$-Ph
20: R_1=OH, R_2=NH-$CH(CH_3)_2$
21: R_1=OH, R_2=NH-$(CH_2)_2$-OH
22: R_1=OH, R_2=NH-2-(1,3-thiazolyl)
23: R_1=OH, R_2= morphinyl
24: R_1=OH, R_2=piperazinyl

Fig. 1 The sulfonamide derivatives coupled with a salicylamide or anisamide scaffold subjected to the present study

more closely than conventionally used cancer monolayer. The tested compounds (**8**–**12**, **15**, and **17**–**19**) were previously shown (Galal et al. 2018) to work as microtubule inhibitors (Fig. 1). Compounds with this mechanism of action are clinically used in treatment of different types of solid tumor Paclitaxel, docetaxel, vincristine, and vinblastine are examples of this class of compounds (Hanauske et al. 1994).

In one spheroid based screening, the majority of active compounds were microtubule inhibitors, indicating that the microtubule assembly is a vulnerable process than can easily be disrupted (Fayad et al. 2011). The same screening pointed out other significant factors that control the efficacy of anticancer compounds, which are their physicochemical properties, lipophilicity, water solubility and pharmacokinetics profile. These factors reflected their ability to penetrate inside tumor mass, and thus exert cytotoxicity on the different tumor layers (Curnis et al. 2002).

Table 1 illustrates the average percentage cytotoxicity of the tested compounds toward breast cancer cell line spheroid (MCF7) and colon cancer cell line spheroid (HCT116) in addition to retinal epithelial cell line spheroid (RPE-1) as a normal human cell in different concentrations. The results showed that the cytotoxicity of all tested compounds is concentration dependent. At 50 µM, compound **9** (5-chloro-*N*-[(*N*-4-chlorophenyl) 4-sulfamoylbenzyl] salicylamide) was the most active among all tested compounds. It showed 70% inhibition on HCT116 spheroids, almost double the activity of cisplatin (36%), and showed higher activity than cisplatin on MCF7 spheroids (32 vs. 25%, respectively). It was significantly toxic to the normal cells spheroids (RPE-1) with 42%, slightly higher than that of cisplatin with 39%. However, in case of HCT116 spheroids, compound **9** is much more toxic to cancer cells than normal cells (70% vs. 42%, respectively). At the lower concentrations used (6.25% and 12.5 µM), compound **9** showed also the best cytotoxicity against HCT116 spheroid (18% and 40%, respectively), while its cytotoxicity against normal cells are very low (7% and 11%, respectively).

Both compound **8** (5-chloro-*N*-[(*N*-phenyl) 4-sulfamoylbenzyl] salicylamide) and compound **12** (5-chloro-*N*-[(*N*-4-methoxyphenyl) 4-sulfamoylbenzyl] salicylamide) showed average percentage cytotoxicity toward MCF7 equal to 22 and 27% at 50 µM, which is as close as that found for cisplatin with near cytotoxicity to the normal cells (38% and 40% vs. 39%, respectively).

On the other hand, compound **11** (5-chloro-*N*-[(*N*-4-methylphenyl) 4-sulfamoylbenzyl] salicylamide) showed good cytotoxicity against HCT116 (41%) comparing with that of cisplatin (36%), while its cytotoxicity towards RPE-1 (33%) is less than that of cisplatin (39%). Compound **18** (5-chloro-*N*-[(*N*-benzyl) 4-sulfamoylbenzyl] salicylamide) and compound **19** (5-chloro-*N*-[(*N*-2-phenylethyl) 4-sulfamoylbenzyl] salicylamide) showed cytotoxicity against

Table 1 The average percentage cytotoxicity of compounds under investigation at different concentrations

		MCF7 sph.		HCT116 sph.		RPE-1 sph.	
	μM	Avg. % CT	SD	Avg. % CT	SD	Avg. % CT	SD
8	6.25	3.73	±1.25	0.78	±2.33	3.55	±3.73
	12.5	4.78	±2.90	1.50	±0.71	6.57	±3.61
	25	10.05	±4.02	23.67	±3.43	13.60	±0.14
	50	21.59	±7.90	25.56	±2.68	38.17	±11.07
9	6.25	5.60	±2.82	18.14	±4.18	7.06	±4.67
	12.5	5.84	±0.62	40.27	±3.75	11.07	±3.83
	25	21.84	±3.79	54.52	±0.54	31.22	±2.94
	50	32.32	±2.67	70.06	±5.15	42.08	±1.51
10	6.25	0.04	±0.72	6.99	±2.65	12.09	±9.95
	12.5	0.19	±0.99	7.38	±6.45	13.91	±4.75
	25	1.10	±1.78	18.40	±6.37	18.92	±3.67
	50	1.98	±1.45	25.73	±7.44	19.57	±2.96
11	6.25	1.03	±7.39	9.34	±2.18	18.02	±5.73
	12.5	1.04	±4.37	13.20	±9.60	21.33	±3.94
	25	2.04	±4.12	28.32	±8.52	22.14	±4.68
	50	2.12	±0.25	41.14	±9.06	32.91	±8.45
12	6.25	2.48	±7.86	14.88	±2.98	4.77	±5.03
	12.5	7.54	±0.22	16.39	±1.07	10.76	±3.96
	25	10.36	±2.64	17.38	±0.54	10.80	±4.98
	50	26.87	±1.47	25.03	±2.24	39.70	±6.17
15	6.25	0.34	±2.94	0.93	±2.57	7.31	±3.66
	12.5	1.66	±3.79	1.73	±0.64	7.87	±2.08
	25	4.33	±2.49	11.16	±9.11	7.92	±2.01
	50	5.02	±2.19	14.57	±0.64	10.20	±1.51
17	6.25	2.29	±7.52	1.90	±1.20	0.81	±1.44
	12.5	3.46	±3.08	1.80	±0.42	2.23	±3.73
	25	4.94	±3.17	0.91	±0.41	5.89	±1.87
	50	6.43	±1.73	16.39	±5.15	6.35	±1.94
18	6.25	0.77	±5.86	2.14	±9.04	0.30	±7.90
	12.5	5.19	±1.79	4.42	±6.86	1.32	±2.58
	25	7.65	±4.03	4.50	±7.80	3.81	±2.66
	50	12.99	±2.94	31.80	±7.84	3.89	±2.07
19	6.25	5.29	±0.54	9.87	±4.72	3.25	±0.43
	12.5	5.97	±1.55	12.98	±4.61	4.47	±5.31
	25	10.07	±4.63	21.77	±7.61	6.14	±1.79
	50	11.69	±15.49	31.32	±8.04	9.58	±1.71
Cisplatin	50	25.32	±3.05	36.42	±5.42	39.41	±6.51

Avg. % CT average percentage of cytotoxicity, *SD* standard deviation, *MCF7 sph*. breast cancer cell line spheroid, *HCT116 sph*. colon cancer cell line spheroid, *RPE-1 sph*. retinal epithelial cell line spheroid

HCT116 slightly lower than that of cisplatin (32% and 31%, respectively) but with much lower cytotoxicity against the normal cells (4% and 10% vs. 39%, respectively).

It is worth to note that it is the first time to report the efficacy of this class of compounds on the 3D model and importance of the multicellular spheroids model for identification of promising anticancer candidate drugs.

Antibacterial and antifungal activities of the selected compounds

In recent years, ligand docking in the binding site of a receptor protein (virtual screening) is one of the most widely techniques used to predict the bioactivity of a set of compounds. The method depends on docking of energy

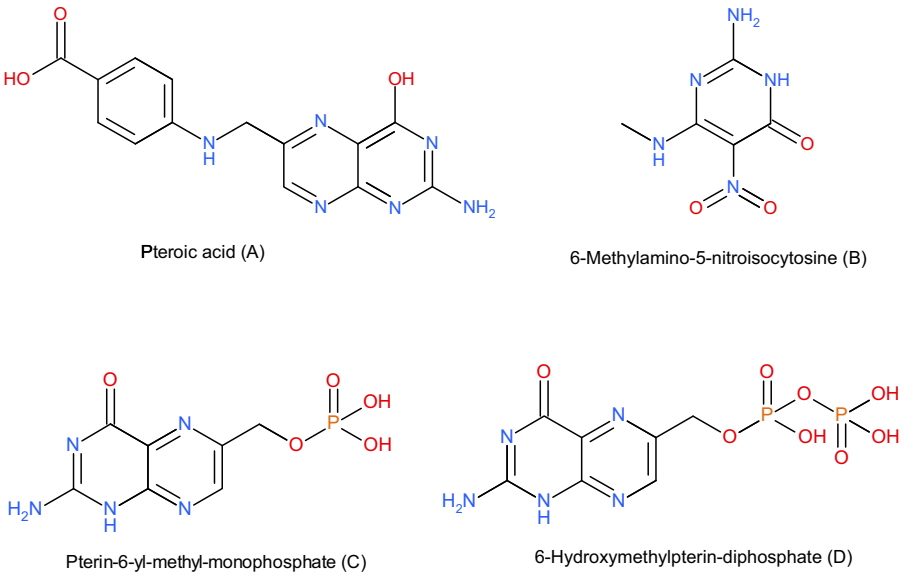

Fig. 2 Chemical structure of the native ligand of the protein IDs: 1TX0, 1TX2, 1TWW, and 1TWZ

Table 2 Hydrogen bonds formed between the native ligand and the surrounded amino acids of the pterin binding pocket

Compounds	Chain A amino acids							Polar contact
	ASP101	ASN120	ASP184	LYS220	ILE122	SER221	HIS256	ARG254
A	√	√	√	√		√		√
B		√	√	√				√
C	√	√	√	√				√
D		√	√	√	√		√	√

minimized 3D ligand structure in the binding set of a definite 3D protein target follows by analysis of the results in comparison with the native ligand.

It was reported that dihydropterate synthase (DHPS) is the target protein for the sulfonamide class of antibiotics and five crystal structures of it were published in the protein data bank IDs 1TX0, 1TX2, 1TWS, 1TWW, and 1TWZ (Babaoglu et al. 2004). Analysis of the pterin binding pocket of the given structures should that it composed of 17 amino acids, GLY64, LYS73, ASP101, ASN120, ILE122, ILE143, MET145, ASP184, GLY188, PHE189, LEU214, GLY216, ARG219, LYS220, SER221, PHE222, ARG254, and HIS256. The native ligands and their hydrogen bonds formed illustrated in Fig. 2 and Table 2, while the secondary structure calculations of chain A and its pterin binding pocket is illustrated in Fig. 3. A virtual screening was carried out using Auto dock Vina software for the sulfonamide derivatives coupled with a salicylamide and/or anisamide scaffold, previously published by us (Galal et al. 2018). The aim of the molecular docking calculations is to predict the promised compounds for resynthesis and testing for their antibacterial and antifungal activities. The docking into the pterin binding pocket, formed hydrogen bonds with the previously mentioned amino acids, binding affinity (kcal mol^{-1}) down −6.5 were considered the basic criteria for

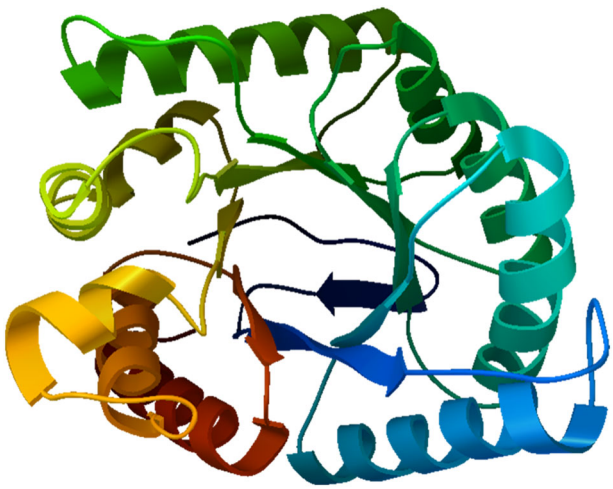

Fig. 3 The secondary structure calculations of chain A and its pterin binding pocket as it was calculated by MGL Tools 1.5.6 (www.mgltools.scripps.edu)

compounds subjected for further study. Table 3 and Fig. 1 illustrated the compounds selected for antibacterial and antifungal test according to the application of the virtual screening.

In vitro, the sulfonamide derivatives were evaluated for their antimicrobial activities against four representative

Table 3 Compounds selected for antibacterial and antifungal test according to the application of the virtual screening

Compound	Binding affinity	Chain A amino acids											
		GLY64	LYS73	ASP101	ASN120	ASP184	SER218	ARG219	LYS220	SER221	ARG234	ARG254	HIS 256
Native ligand	−7.9			√	√	√			√	√		√	
1	−6.5				√							√	
2	−6.5									√	√	√	√
3	−7.1		√	√				√					√
4	−7.2			√						√			√
5	−7.7		√	√				√				√	√
6	−6.6									√		√	√
7	−6.9		√	√			√					√	√
9	−7.2			√									
10	−7.4			√									
12	−7.5			√						√			√
13	−7.5			√									√
14	−7.4	√										√	
16	−7.7			√				√					√
17	−8.0			√				√					√
18	−7.1			√									√
20	−6.7			√	√			√					√
21	−6.9	√		√			√					√	√
22	−7.2				√					√			
23	−7.0				√					√			
24	−7.4				√					√			

Table 4 Inhibition zone of sulfonamide derivatives against G +ve, G −ve bacteria, fungi, and yeast in cm

compounds	Inhibition zone (cm)			
	E. coli	*B. subtilis*	*A. niger*	*C. albicans*
1	0	2.5	0	0
2	0	1.6	0	0
3	0	0	2	0
4	2	2	0	0
5	1	2	3	2
6	0	2.4	0	0
7	0	1.2	0	2.3
9	2	0	1.1	0
10	2.3	0	0	0
12	1.5	0	0	0
13	1.8	0	1.1	0
14	0	2.7	2	0
16	3	0	0	0
17	2.8	3	5	2.5
18	2	0	0	0
20	1	0	0	0
21	2.5	2.7	0	0
22	2	0	0	0
23	1.5	0	0	0
24	2	0	0	0
Control	2.1	2.2	2	3

microbial strains, G +ve bacteria (*Bacillus subtilis* NRRL-B543), G −ve bacteria (*Escherichia coli* NRRL-B210), fungi (*Aspergillus niger* NRRL-599), and yeast (*Candida albicans* NRRL-Y 477). A standard azole drug miconazole for fungi and ceftriaxone for bacteria were used as positive control. Results shown in Table 4 illustrate the antimicrobial activities of the sulfonamide derivatives. It has been found that compound **17** followed by **14**, **21**, **1**, and **6** have the strongest antibacterial activity against the G +ve bacterium (*B. subtilis*) with zone of inhibition 3.0, 2.7, 2.7, 2.5, and 2.4 cm, respectively. While for G −ve bacterium (*E. coli*), compounds **16** followed by **17**, **21**, and **10** showed the highest activity with zone of inhibition 3, 2.8, 2.5, and 2.3 cm, respectively. Compounds **4**, **9**, **18**, **22**, and **24** exhibited the same zone of inhibition against *E. coli*, 2 cm nearly equal to control. Compound **17** followed by compound **5** showed promising antifungal activity on the tested organism (*A. niger*). Compounds **3** and **14** exhibited the same zone of inhibition against *A. niger*, 2 cm equal to control. Concerning the effect of the sulfonamide derivatives on the pathogenic yeast test strain *C. albicans*, it has been found that compounds **17** followed by **7** exhibited lower activities than the control with zone of inhibition (2.5 and 2.3 cm vs. 3 cm, respectively).

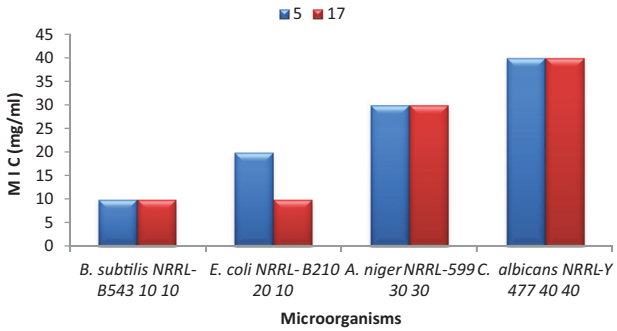

Fig. 4 MIC of compounds **5** and **17** in mg/ml

Table 5 Inhibition zone of **5**, **17**, and their antibiotic synergy at calculated MIC concentrations

Microorganisms	5	17	5(s)*	17(s)*	Control
B. subtilis NRRL-B543	1	1	1.8	1.7	2.2
E. coli NRRL-B210	1.2	1.9	1.1	1.6	2.1
A. niger NRRL-599	2.5	1.7	2	2.2	2
C. albicans NRRL-Y 477	1.7	1.7	2.9	3.4	3

Compound(s)* control antibiotic in equal concentration

Compounds **5** and **17** showed antimicrobial activity on all tested microorganisms, their minimum inhibitory concentration (MIC) were determined in a range from 10 to 40 mg/ml (Fig. 4). The higher activity of compound **17** compared to compound **5** is referred to the hydroxyl group instead of methoxy. Azole drugs works by inhibition of enzymes involved in cell membrane synthesis leads to impair of function and subsequently death of the pathogen (Supuran and Scozzafava 2000), ceftriaxone inhibit cell wall synthesis, while sulfonamides have different mechanism of action. They inhibit folic acid synthesis, which disrupt the DNA synthesis lead to death of the microorganism.

The sulfonamides **5** and **17** exhibited antifungal activity against *A. niger* and *C. albicans* comparable to miconazole, with MICs 30 and 40 mg/ml, respectively.

The synergistic effect between the control antibiotics and both selected compounds were determined (Table 5). Fractional inhibitory concentration (FIC) was calculated for both selected compounds (Table 6). Synergy was defined as an FIC index ≤ 0.5. When the FIC index in range between 0.5 and 4.0 it showed, there was "no interaction" between the agents. FIC > 4.0 indicate there was antagonism between the two agents (Hemaiswarya et al. 2008).

The most potent compounds **5**, **17**, and miconazole, as a standard antifungal inhibitor, were evaluated their capability of inhibiting the DHPS enzyme. As it was displayed in Fig. 5, compound **17** showed strong inhibition (95.15%) than compound **5** (93.78%) as compared to miconazole (87.50%). This results agreed with (McCullough and

Table 6 Fractional inhibitory concentration (FIC) index of compounds **5** and **17**

Microorganisms	FIC 5	FIC 17	FICAntibiotic5	FICAntibiotic17	FICindex5	FICIndex17
B. subtilis NRRL-B543	1.8	1.7	0.8	0.77	2.6	2.47
E. coli NRRL-B210	0.9	0.94	0.5	0.76	1.4	1.7
A. niger NRRL-599	0.8	1.3	1	1.1	1.8	2.7
C. albicans NRRL-Y 477	1.7	2	0.96	1.13	2.66	3.13

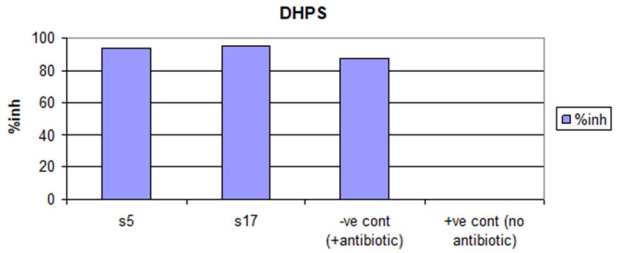

Fig. 5 Effect of **5** and **17** on dihydropterate synthase (DHPS) inhibition

Table 7 Effect of **5** and **17** on lipase and protease inhibition %

Microorganisms	Protease inhibition%		Lipase inhibition%	
	17	5	17	5
B. subtilis NRRL-B543	26	26	75	62.5
E. coli NRRL-B210	8	45	–	43
A. niger NRRL-599	11	33	33	33
C. albicans NRRL-Y 477	–	3	–	–

Maren 1973) who stated that, sulfonamides act as competitive inhibitors of dihydropteroate synthase.

The mechanism of antimicrobial action of both selected compounds seems to be connected with lipase and protease inhibitor activities with different percentage of inhibition (Table 7). The amylase enzyme was not assessed in all tested microorganism (data not shown).

Compounds **17** and **5** showed high lipase inhibition percentage concerning G +ve *B.subtilis* (75% and 62.5%, respectively) and lipase inhibition percentage concerning *A. niger* (33% for both). Compound **5** showed moderate protease inhibition percentage with G-ve *E. coli* and *A. niger* (45% and 33%, respectively). Both compounds inhibited neither yeast *C. albicans* lipase nor protease. Protease inhibition percentage detected by both compounds was coinciding with previously reported on sulfonamide derivatives to exhibit protease inhibitor properties (Supuran et al. 2003). Moreover, protease inhibitors previously reported as anticancer and antiviral agent (Uchima et al. 2004). Where they selectively bind to protease enzyme and inhibit protein precursor that are essentially to production of infection (Shamsi and Fatima 2016).

Lipase enzyme facilitate bacterial colonization in nutrient limited conditions leading to various infectious diseases mainly dermal infections thus drugs targeting inhibit of lipase activity have a powerful curing action (Batubara et al. 2009). Thus, both compounds considered as a new lead antimicrobial compounds.

In silico virtual screening

Virtual screening has gained much interest as a computational tool to expect and select some compounds as target for specific enzyme. The method depends on docking a set of 3D structure of the compounds into the inhibitory pocket of the enzyme and follows by analyzing the results. Applying this method before in vitro measurement leads to save time and money. On the other hand, the increasing of resistance of some microbial strain to most of the antimicrobial drugs encouraged us to investigate the sulfonamide derivatives, previously prepared by us (Galal et al. 2018), as new therapeutic agents against DHPS enzyme. Molecular docking study was carried out using the Auto dock Vina software for the energy minimized 3D structure of the sulfonamide derivatives coupled with a salicylamide or anisamide.

The results obtained were analyzing according to the following criteria:

1. The compound was docked into the pterin pocket.
2. It formed hydrogen bonds with at least two amino acids previously detected for the native ligand (Table 2).
3. It has binding affinity down −6.5 kcal/mol.

Consequently, 20 compounds were selected for the in vitro measurements (Table 3). Figures 6 and 7a represent the most active compounds **5** and **17** docked into the pterin pocket of DHPS enzyme (PDB ID: 1tx0). The electrostatic map potential of the outer most surface of chain A was computed using APBS program (Baker et al. 2001). Figures 6 and 7b represent the hydrogen bonds formed between chain A. Figures 6 and 7c represent the pose view of interaction of compounds **5** and **17** with the amino acids of chain A.

Conclusion

In conclusion, nine of most active sulfonamide derivatives coupled with a salicylamide scaffold were screened for cytotoxicity on two human cancer cell line spheroids (MCF7 and

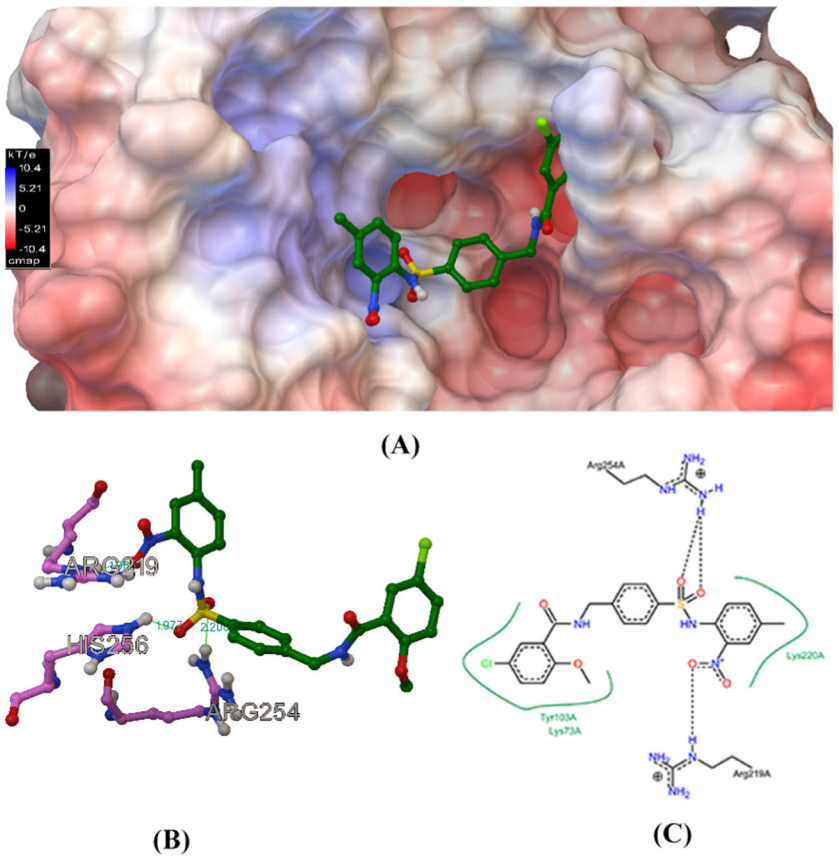

Fig. 6 **a** The binding mode of compound **5** (green) docked into the pterin pocket of DHPS enzyme (chain A, PDB ID: 1tx0). The outer most surface of the protein was illustrated as electrostatic potential map. **b** The 3D binding mode showing compound **5** and its intermolecular hydrogen bonds and bond length (green lines) with ARG219, ARG254 and HIS256 (pink). The compounds colored according to the functional groups. The rest of the enzyme structure was deleted from the view to clarify the docked conformer. **c** 2D of the residues in the active site of DHPS enzyme interacting with compound **5**. The black dashed lines indicate hydrogen bonds, the green solid lines show hydrophobic interactions

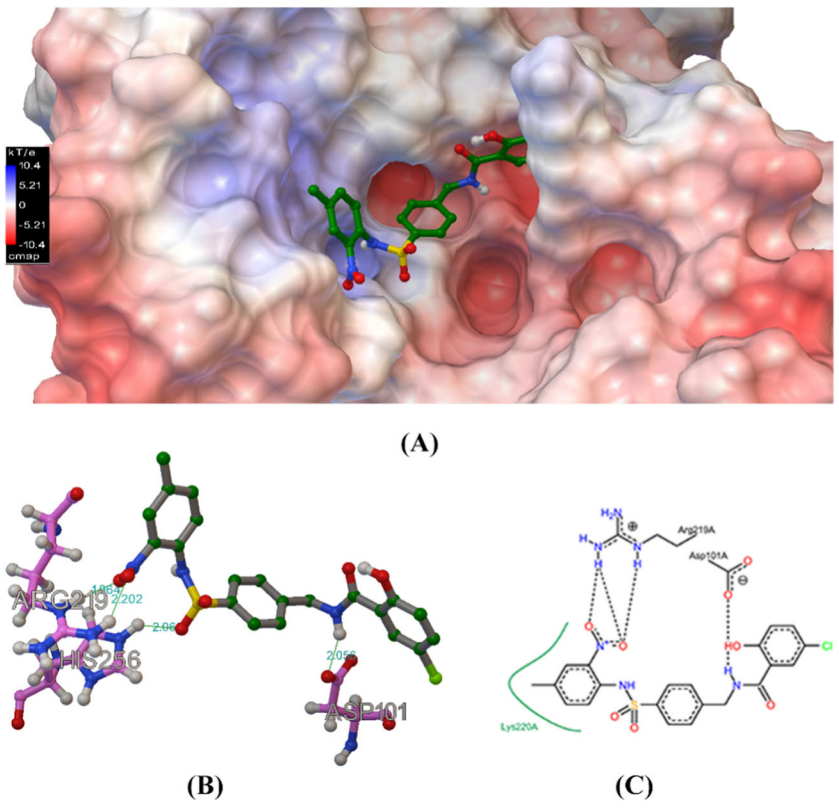

Fig. 7 **a** The binding mode of compound **17** (green) docked into the pterin pocket of DHPS enzyme (Chain A, PDB ID: 1tx0). The outer most surface of the protein was illustrated as electrostatic potential map. **b** The 3D binding mode showing compound **17** and its intermolecular hydrogen bonds and bond length (green lines) with ASP201, ARG219 and HIS256 (pink). The compounds colored according to the functional groups. The rest of the enzyme structure was deleted from the view to clarify the docked conformer. **c** 2D of the residues in the active site of DHPS enzyme interacting with compound **17**. The black dashed lines indicate hydrogen bonds, the green solid lines show hydrophobic interactions

HCT116) in addition to one normal human cell line spheroid (RPE-1). 5-chloro-*N*-[(*N*-4-chlorophenyl) 4-sulfamoylbenzyl] salicylamide (**9**) was found to be the most active compound among all tested compounds. Its activity was found to be almost double the activity of cisplatin toward HCT116 spheroid, while it was little higher toward MCF7 spheroids. In addition, 5-chloro-*N*-[(*N*-benzyl) 4-sulfamoylbenzyl] salicylamide (**18**) and 5-chloro-*N*-[(*N*-2-phenylethyl) 4-sulfamoylbenzyl] salicylamide (**19**) showed cytotoxicity against HCT116 slightly lower than that of cisplatin but with much lower cytotoxicity against the normal cell.

Based on in silico virtual screening against DHPS enzyme, 20 sulfonamide derivatives coupled with a salicylamide and/or anisamide scaffold were tested in vitro against four bacterial and fungal pathogens. 5-Chloro-*N*-[(*N*-2-nitro-4-methylphenyl) 4-sulfamoylbenzyl] salicylamide (**17**) and 5-chloro-*N*-[(*N*-2-nitro-4-methylphenyl) 4-sulfamoylbenzyl] anisamide (**5**) showed strong activity against G +ve bacteria (*B. subtilis*), G −ve bacteria (*E. coli*), fungi (*A. niger*), and yeast (*C. albicans*). In vitro, DHPS enzyme assay showed that compounds **5** and **17** effectively inhibit DHPS enzyme. In addition, their effect upon amylase, lipase and protease enzymes was reported. The most active compounds **5**, **9**, **17–19** could be subjected to in vivo investigation as new drugs.

Experimental

Chemistry

All materials, reagents and solvents were purchased from Sigma-Aldrich, Merck, Fisher chemicals, and Lab-Scan analytical sciences and were used without further purification. ^{1}H and ^{13}C nuclear magnetic resonance (NMR) spectra were recorded at 298 K on a JEOL ECA-500 spectrometer (^{1}H at 500.16 MHz and ^{13}C NMR at 125.76 MHz), and were processed using the Bruker Topspin 3.2 software. ^{1}H and ^{13}C NMR spectra are referenced to ^{1}H signals of residual non-deuterated solvents and ^{13}C signals of the deuterated solvents respectively. ^{1}H NMR signals are reported with chemical shift values δ (ppm), multiplicity (s = singlet, d = doublet, t = triplet, q = quartet, m = multiplet, and br = broad), relative integral, coupling constants J (Hz) and assignments. Mass spectra were recorded on AJEOL DART $^{+}$ HI RESOLUTION mass spectrometer, and ionization of all samples was carried out using ESI. Melting points were measured on an Electro-thermal IA9100 digital melting point apparatus and were uncorrected. Analytic TLC was performed on Merck silica gel 60 F254 precoated aluminum plates (0.2 mm) and visualized under UV light (254 nm).

The compounds under investigation were synthesized according to the method described elsewhere (Galal et al. 2018). The structure of the synthesized compounds was established by mp, HR-MS, and NMR tools.

4-(5-Chloro-2-methoxybenzamido-*N*-methylene) benzene sulfonamide (2)

A mixture of 4-(5-chloro-2-methoxybenzamido-*N*-methylene) benzene sulfonyl chloride (0.88 g, 2.35 mmol) and dry ammonium carbonate powder (3.5 g) was grinding and heated during 30 min. The residue was washed several portions with cold distilled water (15 ml each), filtered off and recrystallized from aqueous methanol to give white powder (**2**; 0.7 g; yield 84%; mp 227–229 °C). ^{1}H-NMR (DMSO-d_6) δ 3.84 (s, 3H, CH_3), 4.51 (d, 2H, $J = 5.75$ Hz, CH_2), 4.77 (br s, 2H, NH_2), 7.12 (s, 1H, Ar-H), 7.27 (t, 1H, $J = 8.6$ Hz, Ar-H), 7.46 (s, 2H, Ar-H), 7.59 (d, 2H, $J = 9.5$ Hz, Ar-H), 7.72 (s, 1H, Ar-H), 8.84 (d, 1H, $J = 9.5$ Hz, NH). ^{13}C-NMR (DMSO-d_6) δ 43.50(C-9), 56.88(C-10), 114.64(C-3), 124.80(C-1), 126.24(C-3',C-5'), 127.02(C-5), 127.92(C-2',C-6'), 130.06(C-6), 132.40(C-4), 140.63(C-1'), 144.17(C-4'), 156.34(C-2), 164.63(C-7). HR-MS (ESI): *m/z* $[M+H]^{+}$calcd. for $C_{15}H_{16}ClN_2O_4S^{+}$ 355.05192 found 355.05177.

Cell culture

All cell lines were kindly provided by Professor Stig Linder, Oncology and Pathology department, Karolinska Institute, Stockholm, Sweden, originally obtained from ATCC. The media for cell growth were as follows: MEM for MCF7, McCoy's 5A for HCT116 and DMEM-F12 for RPE-1. Media were supplemented with 10% fetal bovine serum and 1% penicillin–streptomycin antibiotic. Serum with filtered through 0.45 µm sterile syringe filters to remove particulates that might deform the spheroids. Cells were incubated at 37 °C in 5% CO_2, 95% humidity and subcultured using trypsin versene 0.15%.

Generation of MCS

The spheroids were generated according the centrifugation method (Ivascu and Kubbies 2006). In brief, cell suspension of 10,000 cells/well for MCF7 and HCT116 and 50,000 cells/well for RPE-1 were seeded in poly-HEMA coated 96-round bottom plates and centrifuged for 10 min at 1000*g*. Cells were incubated for 5 days until they form proper spheroids of about 500 µm diameter. Medium was changed day after day.

Cytotoxicity assessment

Compounds were added in triplicates at final concentrations of 6.25, 12.5, 25, and 50 µM. The duration of the treatment

was 7 days. A 50 µM cisplatin was used as a positive control and 0.5% DMSO as a negative control. Cytotoxicity was determined using the acid phosphatase method (Friedrich et al. 2007). After washing twice with 250 µL PBS, spheroids were lysed in 100 µL of 0.1M sodium acetate, 0.1% Triton X- 100, pH 5, *p*-nitrophenyl phosphate (2 mg/ml) (Santa Cruz-Germany) and incubated for 90 min at 37 °C. At the end of the incubation, 10 µL of 1N NaOH stop solution was added to each well and absorbance was measured at 405 nm.

Cytotoxicity was calculated according to the following equation:

$$(1 - (\mathrm{av}(x)/(\mathrm{av}(\mathrm{NC}))) * 100,$$

where av the average, x the absorbance of sample, NC the absorbance of negative control.

In vitro antimicrobial bioassay

Antibacterial activity of sulfonamide derivatives were assessed using well diffusion agar method (Pretorius et al. 2003). Nutrient agar medium was used for growing the G +ve and G −ve bacteria (*B. subtilis* NRRL-B543, *Escherichia coli* NRRL-B210), while potato dextrose agar medium was used for growing of fungi and yeast (*A. niger* NRRL-599 and *C. albicans* NRRL-Y 477). Media were sterilized and inoculated with the test organisms. The optical density of the inoculum was adjusted at 0.125 for freshly grown bacteria and 0.5 for freshly grown yeast and fungi. Wells of 10 mm diameter were punched in each plate. Samples solution of 100 mg sample/ml DMSO was prepared from which 70 µL were added to each well, a negative control well (DMSO only), and reference antimicrobial drug well was made ceftriaxone for bacteria and miconazole for fungi. The plates were incubated for 24 h at 35 °C for bacteria and 28 h at 30 °C for fungi. Antimicrobial activities were evaluated by measuring the inhibition zone diameter (cm).

Minimum inhibitory concentration

Earliest screening showed that compounds **5** and **17** showed activity against all tested organisms. Thus, MIC of both compounds were determined using well diffusion agar method by preparing different concentrations 10, 20, 30, 40 mg/ml of each compound.

Synergy test

The synergy effect between the antibiotics and antimicrobial compounds was determined (Pillai et al. 2005) and combined with calculation of a FIC index (Pei et al. 2009). Synergistic interactions involving the synthetic compounds **5** and **17** (A) plus the reference antibiotic (B). The concentration of the synthetic compound used were their MIC value. The effects of combinations were evaluated by calculating the FIC index for each combination using the following formula: FIC=MIC of drug in combination/MIC of drug alone; FIC index=FIC of drug A+FIC of drug B (Pillai et al. 2005).

Enzymatic activity

In vitro test of DHPS enzyme inhibition

The most potent compounds **5** and **17** were subjected to the DHPS enzyme assay to check their efficiency to suppress 7,8-dihydropteroate process in the folate biosynthesis. Totally, 50 µl of MIC concentration (30 mg/ml) of compounds **5** and **17** were separately prepared in DMSO and incubated with cell extract of *A. niger* NRRL-599 grown on broth dox media for 48 h. miconazole with the same concentration range was used as positive control against *A. niger* NRRL-599. Then, 100 µl of lysate (100 µg of protein) was combined with ^{14}C-labeled *PABA*, diphosphoric acid, and mono[(2-amino1,4,7,8-tetrahydro-4-oxo-6-pteridinyl)-methyl]ester in Tris buffer, pH 8.3, containing dithiothreitol and $MgCl_2$ in a 200 µl reaction volume, and the mixture was held at 37 °C for 15 min. One hundred microliters of each reaction volume was spotted onto 3 MM paper (Whatman International, Ltd., Maidstone, England), and ascending chromatography was performed in 0.01 M phosphate buffer. Under these conditions, free substrate (^{14}C-labeled *PABA*) migrates with the solvent front and radiolabeled product (^{14}C-labeled dihydropteroate) remains at the origin. The chromatogram was dried, the area (1 cm^2) representing the origin was placed into scintillation fluid, and radioactivity was measured using an LS 6000IC Liquid Scintillation System (Beckman Instruments, Fullerton, CA). Results were expressed as the mean and standard deviation of triplicate samples in picomoles of product formed per milligram of total protein (Ho et al. 1975).

Amylase enzyme

Fungal amylase

The fungus was grown in 25 ml of media composed of g/L: ($NaNO_3$, 3 g; $MgSO_4.7H_2O$, 0.5 g; KCl, 5 g; KH_2PO_4,1 g; $FeSO_4{\cdot}7H_2O$, 0.01 g; $CaCl_2$, 0.1 g); starch, 15 g in 150 ml Erlenmeyer flasks and autoclaved at 121 °C for 15 min. After sterilization, the flasks were cooled to room temperature. Totally, 0.1 ml spore suspension of the fungal strain (OD 0.5) was inoculated and MIC concentration of selected compound was added (the control without selected compound) and incubated for 3 days (Sunitha et al. 2012).

Bacterial amylase

A loop full of bacterial culture was transferred from starch-nutrient agar slants to starch-nutrient broth at pH 7 for activation and incubated in a shaker at 40 °C at 120 rpm for 24 h. Fermentation medium composed of g/L: soluble starch, 10 g; peptone, 5 g; $(NH_4)_2$ SO_4, 2 g; KH_2PO_4, 1 g; K_2HPO_4, 2 g; $MgCl_2$, 0.01 g; at pH 7. The fermentation medium was inoculated with the activated culture (20% v/v). Selected compound (MIC concentration) was added to the inoculated media (the control without selected compound) and incubated in a shaker at 37 °C for 24 h. At the end of the fermentation period, the culture medium was centrifuged at 10,000 rpm for 15 min to obtain the crude extract, which served as enzyme source (Vaidya and Rathore 2015).

Lipase enzyme

Fungal lipase For lipase production, the composition of the medium used was (g% w/v), glucose,1; olive oil, 1; peptone, 30; KH_2PO_4, 0.2; KCl, 0.05; $MgSO_4{\cdot}7H_2O$, 0.05; at pH 6. The medium was heat sterilized at 121 °C for 15 min. Inoculated with 5 ml spore suspension (OD 0.5) (Mostafa and El-Hadi 2010). MIC concentration of selected compound was added to inoculated medium (the control without selected compound) and incubated for 3 days at 30 °C.

Bacterial lipase For lipase production, the composition of the medium used was (g% w/v) yeast extract, 0.3; peptone, 0.1; olive oil, 1; K_2HPO_4, 0.07; KH_2PO_4, 0.03; $MgSO_4$, 0.05; $MnCl_2$, 0.01; $(NH_4)_2SO_4$, 0.025 and $CaCl_2$, 0.01. The flasks were inoculated with bacterial suspension (OD 0.125). MIC concentration of selected compound was added (the control without selected compound) and incubated at 35 °C with a constant shaking at 125 rpm for 2 days. The cells were separated by centrifugation at 10,000 rpm and 4 °C for 20 min (Zouaoui and Bouziane 2011).

Protease enzyme

Fungal protease

The medium used for protease production was composed of (g/L): $CaCl_2{\cdot}7H_2O$, 0.4; KH_2PO_4, 7.0; Na_2HPO_4, 2.5; $MgSO_4{\cdot}7H_2O$, 0.5; $ZnCl_2$, 0.1; NaC1, 0.3; Casein, 2.0; pH 6.0. Media were autoclaved at 120 °C for 20 min (Ali et al. 1998). Inoculated with 5 ml spore suspension (OD 0.5) and selected compound (MIC concentration) was added (the control without selected compound) and incubated for 3 days.

Bacterial protease

The medium used for protease production was composed of (g/L): nutrient broth with NaCl, 0.5 g; casein, 0.1 g; pH 7.0. Media were autoclaved at 120 °C for 20 min. Inoculated with (1%) inoculums. MIC concentration of selected compound was added (the control without selected compound) and kept for 24 h incubation at 37 °C under shaking condition of 150 rpm. After incubation, the culture was centrifuged at 10,000 rpm for 15 min at 4 °C (Suganthi et al. 2013).

Assay of amylase enzyme

Total amylase activity (TAA) was determined (Murado et al. 1993) by mixing 80 µL of cell-free medium with 400 µL of 0.15 M citrate–phosphate buffer; pH 5.0 (1 volume) and 4% soluble starch (1.5 volumes) previously maintained at 40 °C/15 min. The reaction mixture was incubated at 40 °C for 10 min. The reaction was stopped by addition of 480 µL of dinitrosalicylic acid. One unit of amylase activity (enzymatic units (EU)/ml) was defined as the amount of enzyme that releases 1 mg/ml of reducing sugars (glucose equivalents) under the assay conditions.

Assay of lipase enzyme

Lipase was performed with olive oil emulsion as follows: 10 ml olive oil and 90 ml of 10% arabic gum were emulsified by a homogenizer for 6 min at 20.000 rev/min The reaction mixture composed of 3 ml olive oil emulsion, 1 ml 0.2 M tris-buffer (pH 7.5), 2.5 ml distilled water and 1 ml enzyme solution were incubated at 37 °C for 2 h with shaking. The emulsion was destroyed by addition of 10 ml acetone (95% v/v) immediately after incubation, and liberated free fatty acids were titrated with 0.05 N NaOH. One unit of lipase was refined as the amount of enzyme liberated 1 µmol of fatty acids (Mostafa and El-Hadi 2010).

Assay of protease enzyme

Protease activity in the crude enzyme extract was determined (Cupp-Enyard 2008) by using casein as substrate. Two test tubes were taken and labeled as test (T) and blank (B). A 5 ml of 0.65% casein solution was added in test and blank tubes and test tubes were placed at 37 °C for 5 min. One milliliter of enzyme solution was added in T-test tube. It was mixed properly and incubated at 37 °C in a water bath for 30 min for allowing the enzymatic reaction to occur. The reaction was terminated by addition of 5 mL of 15% trichloroacetic acid solution in both test and blank tubes. One milliliter of enzyme solution was added in blank test tube only and it was allowed to stand for 15 min at room

temperature. Solution from both test tubes was filtered using Whatmann no. 1 filter paper. Two milliliter of test and blank filtrate were taken in two new test tubes and labeled as test (T) and blank (B). Five milliliter of sodium carbonate was added in both test tubes followed by addition of 1 ml of 2-fold diluted Follin Ciocalteus phenol reagent. The resulting solutions in both test tubes were incubated for 30 min at room temperature in dark, for the development of blue color. The absorbance of the blue color compound was measured at 660 nm against a reagent blank using tyrosine standard. One protease unit was defined as the amount of enzyme that releases 1 µM of tyrosine per minute (Mohapatra et al. 2003).

Molecular docking

The X-ray diffraction of the protein 1tx0 with resolution 2.15 Å was downloaded from the protein data bank (http://www.rcsb.org/pdb/welcome.do). Its energy was minimized using the YASARA Energy Minimization Server (http://www.rcsb.org/pdb/welcome.do), all bound water, ligands, and cofactors were removed. The pdbqt file format of the protein and the synthesized compounds were created using MGL Tools 1.5.6 (www.mgltools.scripps.edu). Docking calculations were performed using Auto Dock Vena (Trott and Olson 2010) and PyRx 0.8 (www.mgltools.scripps.edu). The results were analyzed based on the binding of the ligand at the inhibitory pocket using PyMol 1 (www.pymol.org).

Future perspective

The present study explored the cytotoxic activity of some sulfonamide derivatives coupled with a salicylamide scaffold compounds against human cancer cell line spheroids. The most active compounds **9**, **18**, and **19** will be subjected to in vivo studies to evaluate their activities, safety and the side effects. In addition, it sheds light on the important of compounds **5** and **17** as antibacterial and antifungal compounds that can be developed to be drugs after intensive biostudies.

Acknowledgements We are grateful for Professor Stig Linder, Karolinska Institute, Sweden, for kindly providing us with HCT116, MCF7, and RPE1 cell lines.

Compliance with ethical standards

Conflict of interest The authors declare that they have no conflict of interest.

References

Ali A, Reddy GS, Cao H, Anjum SG, Nalam MN, Schiffer CA, Rana TM (2006) Discovery of HIV-1 protease inhibitors with picomolar affinities incorporating *N*-aryl-oxazolidinone-5-carboxamides as novel P2 ligands. J Med Chem 49(25):7342–7356

Ali AI, Ogbonna CC, Rahman AT (1998) Hydrolysis of certain Nigerian starches using crude fungal amylase. Niger J Biotechnl 9:24–36

Babaoglu K, Qi J, Lee RE, Whilte SW (2004) Crystal structure of 7,8-dihydropteroate synthase from *Bacillus anthracis*: mechanism and novel inhibitor design. Structure 12(9):1705–1717

Baker BM, Chen CS (2012) Deconstructing the third dimension: how 3D culture microenvironments alter cellular cues. J Cell Sci 125 (Pt 13):3015–3024

Baker NA, Sept D, Joseph S, Holst MJ, McCammon JA (2001) Electrostatics of nanosystems: application to microtubules and the ribosome. Proc Natl Acad Sci USA 98(18):10037–10041

Batubara I, Mitsunaga T, Ohashi H (2009) Screening antiacne potency of Indonesian medicinal plants: antibacterial, lipase inhibition, and antioxidant activities. J Wood Sci 55:230–235

Bertacine Dias MV, Santos JC, Libreros-Zúñiga GA, Ribeiro JA, Chavez-Pacheco SM (2018) Folate biosynthesis pathway: mechanisms and insights into drug design for infectious diseases. Future Med Chem 10(8):935–959

Chiarino D, Napoletano M, Sala A (1988) Synthesis of 4,7-dihydro-4-oxoisoxazolo[5,4-b]pyridine-5-carboxylic acid derivatives as potential antimicrobial agents. J. Heterocyclic Chem 25 (1):231–233

Cupp-Enyard C (2008) Sigma's non-specific protease activity assay—casein as a substrate. J Vis Exp 19:899

Curnis F, Sacchi A, Corti A (2002) Improving chemotherapeutic drug penetration in tumors by vascular targeting and barrier alteration. J Clin Invest 110(4):475–482

Davie BJ, Christopoulos A, Scammells PJ (2013) Development of M1 mAChR allosteric and bitopic ligands: prospective therapeutics for the treatment of cognitive deficits. ACS Chem Neurosci 4 (7):1026–1048

Ekert JE, Johnson K, Strake B, Pardinas J, Jarantow S, Perkinson R, Colter DC (2014) Three-dimensional lung tumor microenvironment modulates therapeutic compound responsiveness in vitro–implication for drug development. PLoS One 9(3):e92248

Fayad W, Rickardson L, Haglund C, Olofsson MH, D'Arcy P, Larsson R, Linder S, Fryknas M (2011) Identification of agents that induce apoptosis of multicellular tumor spheroids: enrichment for mitotic inhibitors with hydrophobic properties. Chem Biol Drug Des 78(4):547–557

Friedrich J, Eder W, Castaneda J, Doss M, Huber E, Ebner R, Kunz-Schughart LA (2007) A reliable tool to determine cell viability in complex 3-d culture: the acid phosphatase assay. J Biomol Screen 2(7):925–937

Galal AMF, Shalaby EM, Abouelsayed A, Ibrahim MA, Al-Ashkar E, Hanna AG (2018) Structure and absolute configuration of some 5-chloro-2-methoxy-*N*-phenylbenzamide derivatives. Spectrochim Acta A Mol Biomol Spectrosc 188:213–221

Galal AMF, Soltan MM, Ahmed ER, Hanna AG (2018) Synthesis and biological evaluation of novel 5-chloro-*N*-(4-sulfamoylbenzyl) salicylamide derivatives as tubulin polymerization inhibitors. MedChemComm 9(9):1511–1528

Galateanu B, Hudita A, Negrei C, Ion RM, Costache M, Stan M, Nikitovic D, Hayes AW, Spandidos DA, Tsatsakis AM, Ginghina O (2016) Impact of multicellular tumor spheroids as an in vivo-like tumor model on anticancer drug response. Int J Oncol 48 (6):2295–2302

Galiana-Roselló C, Bilbao-Ramos P, Dea-Ayuela MA, Rolón M, Vega C, Bolas-Fernández F, Garcia-España E, Alfonso J, Coronel C, Gonzlez- Rosende ME (2013) In vitro and in vivo antileishmanial and trypanocidal studies of new *N*-benzene- and *N*-naphthalene-sulfonamide derivatives. J Med Chem 56(22):8984–8998

Gangjee A, Kurup S, Namjoshi O (2007) Dihydrofolate reductase as a target for chemotherapy in parasites. Curr Pharm Des 13 (6):609–639

Hanan EJ, Fucini RV, Romanowski MJ, Elling RA, Lew W, Purkey HE, Vanderporten EC, Yang W (2008) Design and synthesis of 2-amino-isoxazolopyridines as Polo-like kinase inhibitors. Bioorg Med Chem Lett 18(19):5186–5189

Hanauske AR, Depenbrock H, Shirvani D, Rastetter J (1994) Effects of the microtubule-disturbing agents docetaxel (Taxotere), vinblastine and vincristine on epidermal growth factor-receptor binding of human breast cancer cell lines in vitro. Eur J Cancer 30A(11):1688–1694

Hanson AD, Gregory III JF (2011) Folate biosynthesis, turnover, and transport in plants. Annu Rev Plant Biol 62:105–125

Hawser S, Lociuro S, Islam K (2006) Dihydrofolate reductase inhibitors as antibacterial agents. Biochem Pharmacol 71(7):941–948

Hay M, Thomas DW, Craighead JL, Economides C, Rosenthal J (2014) Clinical development success rates for investigational drugs. Nat Biotechnol 32(1):40–51

Hemaiswarya S, Kruthiventi AK, Doble M (2008) Synergism between natural products and antibiotics against infectious diseases. Phytomedicine 15(8):639–652

Ho RI, Corman L, Mores SA, Schneider H (1975) Structure-activity of sulfones and sulfonamides on dihydropteroate synthetase from *Neisseria meingitidis*. Antimicrob Agents Chemother 7 (6):758–763

Höhn H, Polacek I, Schulze E (1973) Potential antidiabetic agents. Pyrazolo(3,4-b)pyridines. J Med Chem 16(12):1340–1346

Ivascu A, Kubbies M (2006) Rapid generation of single-tumor spheroids for high-throughput cell function and toxicity analysis. J Biomol Screen 11(8):922–932

Keche AP, Hatnapure GD, Tale RH, Rodge AH, Birajdar SS, Kamble VM (2012) A novel pyrimidine derivatives with aryl urea, thiourea and sulfonamide moieties: synthesis, anti-inflammatory and antimicrobial evaluation. Bioorg Med Chem Lett 22 (10):3445–3448

Kim TH, Mount CW, Gombotz WR, Pun SH (2010) The delivery of doxorubicin to 3-D multicellular spheroids and tumors in a murine xenograft model using tumor-penetrating triblock polymeric micelles. Biomaterials 31(28):7386–7397

Kimlin LC, Casagrande G, Virador VM (2013) In vitro three-dimensional (3D) models in cancer research: an update. Mol Carcinog 52(3):167–182

Kobayashi H, Man S, Graham CH, Kapitain SJ, Teicher BA, Kerbel RS (1993) Acquired multicellular-mediated resistance to alkylating agents in cancer. Proc Natl Acad Sci USA 90 (8):3294–3298

Lee GY, Kenny PA, Lee EH, Bissell MJ (2007) Three-dimensional culture models of normal and malignant breast epithelial cells. Nat Methods 4(4):359–365

Lee HY, Pan SL, Su MC, Liu YM, Kuo CC, Chang YT, Wu JS, Nien CY, Mehndiratta S, Chang CY, Wu SY, Lai MJ, Chang JY, Liou JP (2013) Furanylazaindoles: potent anticancer agents in vitro and in vivo. J Med Chem 56(20):8008–8018

Lee J, Cuddihy MJ, Kotov NA (2008) Three-dimensional cell culture matrices: state of the art. Tissue Eng Part B Rev 14(1):61–86

McCullough JL, Maren TH (1973) Inhibition of dihydropteroate synthase from *Escherichia coli* by sulfones and sulfonamides. Antimicrob Agents Chemother 3(6):665–669

McGuire JJ (2003) Anticancer antifolates: current status and future directions. Curr Pharm Des 9(31):2593–2613

Mohan R, Banerjee M, Ray A, Manna T, Wilson L, Owa T, Bhattacharyya B, Panda D (2006) Antimitotic sulfonamides inhibit microtubule assembly dynamics and cancer cell proliferation. Biochemistry 45(17):5440–5449

Mohapatra BR, Bapuji M, Sree A (2003) Production of industrial enzymes (amylase, carboxymethylcellulase and protease) by bacteria isolated from marine sedentary organisms. Acta Biotechnol 23(1):75–84

Mostafa H, El-Hadi AA (2010) Immobilization of *Mucor racemosus* NRRL 3631 lipase with different polymer carriers produced by radiation polymerization. Malay J Microbiol 6(2):149–155

Murado MA, Siso MaIG, Gonzalez MaP, Montemayor MI, Pastrana L, Miron J (1993) Characterization of microbial biomasses and amylolytic preparations obtained from mussel processing waste treatment. Bioresource Technol 43(2):117–125

Owa T, Yokoi A, Yamazaki K, Yoshimatsu K, Yamori T, Nagasu T (2002) Array-based structure and gene expression relationship study of antitumor sulfonamides including *N*-[2-[(4-hydroxyphenyl)amino]-3-pyridinyl]-4-methoxybenzenesulfonamide and *N*-(3-chloro-7-indolyl)-1,4-benzenedisulfonamide. J Med Chem 45(22):4913–4922

Owa T, Yoshino H, Okauchi T, Yoshimatsu K, Ozawa Y, Sugi N, Nagasu T, Koyanagi N, Kitoh K (1999) Discovery of novel antitumor sulfonamides targeting G1 phase of the cell cycle. J Med Chem 42(19):3789–3799

Pei RS, Zhou F, Ji BP, Xu J (2009) Evaluation of combined antibacterial effects of eugenol, cinnamaldehyde, thymol, and carvacrol against *E. coli* with an improved method. J Food Sci 74(7): M379–M383

Pillai SK, Moellering RC, Eliopoulos GM (2005) Antimicrobial combinations. In: Lorian V (ed) Antibiotics in laboratory medicine, 5th ed. Lippincott Williams & Wilkins, Philadelphia, p 365–440

Poręba K, Pawlik K, Rembacz KP, Kurowska E, Matuszyk J, Długosz A (2015) Synthesis and antibacterial activity of new sulfonamide isoxazolo[5,4-b]pyridine derivatives. Acta Pol Pharm 72 (4):727–735

Pretorius JC, Magama S, Zietsman PC, van Wyk BE (2003) Growth inhibition of plant pathogenic bacteria and fungi by extracts from selected South African plant species. South African J Botany 69 (2):186–192

Procopiou PA, Barrett JW, Barton NP, Begg M, Clapham D, Copley RCB, Ford AJ, Graves RH, Hall DA, Hancock AP, Hill AP, Hobbs H, Hodgson ST, Jumeaux C, Lacroix YML, Miah AH, Morriss KML, Needham D, Sheriff EB, Slack RJ, Smith CE, Sollis SL, Staton H (2013) Synthesis and structure-activity relationships of indazole arylsulfonamides as allosteric CC-chemokine receptor 4 (CCR4) antagonists. J Med Chem 56 (5):1946–1960

Shamsi TN, Fatima S (2016) Protease inhibitors as ad-hoc antibiotics. Open Pharma Sci J 3:131–137

Smith SJ, Wilson M, Ward JH, Rahman CV, Peet AC, Macarthur DC, Rose FR, Grundy RG, Rahman R (2012) Recapitulation of tumor heterogeneity and molecular signatures in a 3D brain cancer model with decreased sensitivity to histone deacetylase inhibition. PLoS One 7(12):e52335

Suganthi C, Mageswari A, Karthikeyan S, Anbalagan A, Sivakumar K, Gothandam M (2013) Screening and optimization of protease production from a halotolerant *Bacillus licheniformis* isolated from saltern sediments. J Gen Eng Biotechnol 11(1):47–52

Sunitha VH, Ramesha A, Savitha J, Srinivas C (2012) Amylase production by endophytic fungi *Cylindrocephalum* sp. isolated from medicinal plant *Alpinia calcarata* (Haw.) Roscoe. Braz J Microbiol 43(3):1213–1221

Supuran CT, Casini A, Scozzafava A (2003) Protease inhibitors of the sulfonamide type: anticancer, antiinflammatory, and antiviral agents. Med Res Rev 23(5):535–558

Supuran CT, Scozzafava A (2000) Carbonic anhydrase inhibitors: aromatic sulfonamides and disulfonamides act as efficient tumor growth inhibitors. J Enzyme Inhib 15(6):597–610

Supuran CT, Scozzafava A, Clare BW (2002) Bacterial protease inhibitors. Med Res Rev 22(4):329–372

Sutherland RM, McCredie JA, Inch WR (1971) Growth of multicell spheroids in tissue culture as a model of nodular carcinomas. J Natl Cancer Inst 46(1):113–120

Tang YB, Lu D, Chen Z, Hu C, Yang Y, Tian JY, Ye F, Wu L, Zhang ZY, Xiao Z (2013) Design, synthesis and insulin-sensitising effects of novel PTP1B inhibitors. Bioorg Med Chem Lett 23 (8):2313–2318

Tannock IF, Lee CM, Tunggal JK, Cowan DS, Egorin MJ (2002) Limited penetration of anticancer drugs through tumor tissue: a potential cause of resistance of solid tumors to chemotherapy. Clin Cancer Res 8(3):878–884

Trott O, Olson AJ (2010) AutoDock Vina: improving the speed and accuracy of docking with a new scoring function, efficient optimization, and multithreading. J Comput Chem 31 (2):455–461

Tunggal JK, Cowan DS, Shaikh H, Tannock IF (1999) Penetration of anticancer drugs through solid tissue: a factor that limits the effectiveness of chemotherapy for solid tumors. Clin Cancer Res 5:1583–1586

Uchima Y, Sawada T, Nishihara T, Maeda K, Ohira M, Hirakawa K (2004) Inhibition and mechanism of action of a protease inhibitor in human pancreatic cancer cells. Pancreas 29(2):123–131

Vaidya S, Rathore P (2015) Isolation, screening and characterization of amylase producing bacteria from soil of potato dump sites from different regions of madhya pradesh. Conference Paper

Wallace DI, Guo X (2013) Properties of tumor spheroid growth exhibited by simple mathematical models. Front Oncol 3:51

Weidel E, de Jong JC, Brengel C, Storz MP, Braunshausen A, Negri M, Plaza A, Steinbach A, Müller R, Hartmann RW (2013) Structure optimization of 2-benzamidobenzoic acids as PqsD inhibitors for *Pseudomonas aeruginosa* infections and elucidation of binding mode by SPR, STD NMR, and molecular docking. J Med Chem 56(15):6146–6155

Wenzel C, Riefke B, Gründemann S, Krebs A, Christian S, Prinz F, Osterland M, Golfier S, Räse S, Ansari N, Esner M, Bickle M, Pampaloni F, Mattheyer C, Stelzer EH, Parczyk K, Prechtl S, Steigemann P (2014) 3D high-content screening for the identification of compounds that target cells in dormant tumor spheroid regions. Exp Cell Res 323(1):131–143

Wilkinson BL, Bornaghi LF, Wright AD, Houston TA, Poulsen SA (2007) Anti-mycobacterial activity of a bis-sulfonamide. Bioorg Med Chem Lett 17(5):1355–1357

Zanoni M, Piccinini F, Arienti C, Zamagni A, Santi S, Polico R, Bevilacqua A, Tesei A (2016) 3D tumor spheroid models for in vitro therapeutic screening: a systematic approach to enhance the biological relevance of data obtained. Sci Rep 6:19103

Zouaoui B, Bouziane A (2011) Isolation, optimisation and purification of lipase production by *Pseudomonas Aeruginosa*. J Biotechnol Biomater 1:120